Tunable 3–6 THz Polariton Laser Exceeding 0.1 mW Average Output Power Based on Crystalline $RbTiOPO_4$

Tiago A. Ortega, Helen M. Pask, David J. Spence, and Andrew J. Lee

***Abstract*—We report a diode-pumped, intracavity THz laser source based on stimulated polariton scattering in crystalline $RbTiOPO_4$ using a surface-emitting configuration. The system was continuously tunable in four regions, from 3.05 to 3.16 THz, from 3.50 to 4.25 THz, from 4.57 to 4.75 THz, and from 5.40 to 5.98 THz. The laser delivered 124.7 μW average output power at 4.10 THz for only 6.0 W diode pump power at 808 nm, corresponding to a diode-to-THz conversion efficiency of 2.1×10^{-5}. The horizontal and vertical beam quality parameters were $M_H^2 < 1.6$ and $M_V^2 < 1.1$ and the linewidth of the terahertz field was 28 GHz at 4.10 THz. The results demonstrate that the surface-emitting configuration is a very efficient technique to produce high-power THz laser sources with frequency-tunable output suitable for real-world applications.**

***Index Terms*—Nonlinear optics, parametric devices, Raman scattering, solid-state lasers, stimulated polariton scattering (SPS), terahertz lasers.**

I. Introduction

TERAHERTZ spectroscopy and spectral imaging techniques have demonstrated great potential to address important real-world applications in various fields, particularly in medicine [1]–[3], homeland security [4]–[6] and nondestructive testing across a wide range of industries [7]–[9]. However, further development of robust, reliable and cost-effective THz sources with sufficient output power is crucial to produce commercially viable systems.

A prominent technique for THz generation is stimulated polariton scattering (SPS) which has been demonstrated in nonlinear crystals such as $MgO:LiNbO_3$ (MgO:LN), $KTiOPO_4$ (KTP), $KTiOAsO_4$ (KTA), and more recently $RbTiOPO_4$ (RTP) [10]–[15]. In SPS, a fundamental laser field (frequency ν_{f}) interacting with a polariton mode of a nonlinear crystal parametrically generates two other fields, a Stokes (frequency ν_{S}) and a polariton field (with terahertz frequency ν_{THz}), in a noncollinear phase matching configuration [10]. The frequency of the polariton field is the difference between ν_{f} and ν_{S}, in keeping with the conservation of energy. To satisfy momentum conservation, a noncollinear phase matching scheme is used, and the frequency of the Stokes and THz fields can be modified by adjusting the interaction angle between the fundamental and Stokes fields [10].

A key design consideration for SPS lasers is how to efficiently extract the generated terahertz radiation from the crystal. Here there are two key challenges. First, strong THz absorption by the nonlinear material makes it necessary to minimize the length over which the THz field must propagate before exiting the crystal. Second, the high refractive indices for THz radiation can lead to total internal reflection (TIR) if the angle of incidence of the THz beam exceeds the critical angle. For this reason high-resistivity silicon prisms are typically bonded to the crystal's side face, enabling the THz radiation to refract into the silicon and exit the prisms at near-normal incidence, into the air [16]. There are substantial Fresnel reflection losses and significant absorption of the THz field during its propagation through the silicon prisms. A more efficient extraction mechanism is the surface-emitting (SE) configuration, in which the fundamental and Stokes fields experience TIR inside the nonlinear crystal, and the phase matching angles result in a polariton field generated in close proximity and at near-normal incidence to the crystal-air interface. Hence, the THz radiation generated at the TIR surface is refracted directly into the air. The SE configuration has been reported using several polariton crystals including MgO:LN, KTP and KTA [13], [14], [17] where it was found to be effective at producing higher THz outputs and smaller beam sizes when compared to the performance of linear resonators in combination with silicon prisms.

SPS has been demonstrated for externally-pumped and intracavity nonlinear crystals. Reaching SPS threshold for externally-pumped crystals however, require the use of high energy pulsed laser systems, which are generally complex, often expensive and lack compactness. This can be contrasted to the intracavity design, in which the SPS crystal is placed inside the resonator of what is typically a diode-pumped Nd laser, making use of the intense intracavity fields to reach SPS threshold for very modest (typically a few Watts at 808 nm) diode pump powers [18]. The resulting devices are typically compact and cost-effective, and can be pumped by conventional laser diodes.

Manuscript received November 14, 2017; revised January 25, 2018 and February 22, 2018; accepted February 22, 2018. Date of publication February 28, 2018; date of current version March 15, 2018. This work was supported by the Australian Research Council through the Discovery Project Scheme (DP11013748), Linkage Project Scheme (LP140100724), and Future Fellowship Scheme (Pask, FT120100294). *(Corresponding author: Tiago A. Ortega.)*

The authors are with the MQ Photonics Research Centre, Department of Physics and Astronomy, Macquarie University, Sydney, N.S.W. 2109, Australia (e-mail: tiago.ortega@students.mq.edu.au; helen.pask@mq.edu.au; david.spence@mq.edu.au; andrew.lee@mq.edu.au).

Color versions of one or more of the figures in this paper are available online at http://ieeexplore.ieee.org.

Digital Object Identifier 10.1109/JSTQE.2018.2810380

They exhibit very low SPS threshold, high average THz output powers and outstanding diode-to-THz efficiency when compared with externally pumped systems [12], [18]. Most intracavity SPS terahertz lasers have used MgO:$LiNbO_3$ to generate terahertz fields continuously tunable in the ~1–3 THz range in both linear [18], [19] and SE configurations [20], [21]. Recently, our group sought to extend the THz frequency coverage of these sources, and reported the first intracavity SPS source based on a different nonlinear material, RTP, which was implemented in a linear configuration[15].

Rubidium titanyl phosphate (RTP) is an excellent nonlinear crystal widely used in electro-optical devices, due to its high nonlinear coefficient, high laser damage threshold, low-switching voltage and high transparency range [22]. These attributes make RTP a very attractive material for SPS, and the system reported in [15] produced detectable terahertz radiation ranging from 3.10–4.15 THz, with a maximum average output power of 16.2 μW at 3.80 THz. However, while the Stokes lasing indicated THz fields up to 7.05 THz were being generated inside the material, no emission above 4.15 THz could be detected, and this was attributed to increased THz extraction losses and reduced detection efficiencies associated with the higher THz frequencies. The use of an intracavity RTP crystal in a SE configuration was proposed as a potential means for increasing the range of THz frequencies that could be detected.

In this manuscript we report, for the first time to our knowledge, a THz polariton laser based on an intracavity RTP in a surface-emitting configuration which produces terahertz radiation in four tunable bands between 3.05 THz and 5.98 THz, providing much better spectral coverage compared to the 3.10–4.15 THz reported previously using a linear configuration [15]. The lack of continuous tunability is associated with infrared absorbing modes in the material [15]. Moreover, the SE configuration promoted a substantial increase of more than 7 times in THz output power and in one order of magnitude in diode-to-THz efficiency. A maximum average output power of 124.7 μW was detected at 4.10 THz for a diode pump power of just 6 W, resulting in a diode-to-THz efficiency of 2.1×10^{-5}. This result represents an important milestone because it is not only the highest average THz output power and diode-to-THz efficiency ever reported for any intracavity SPS laser, but also the first time an intracavity SPS source has exceeded the 0.1 mW average output power level.

II. Experimental Details

The THz polariton laser with the intracavity RTP crystal in SE configuration is outlined in Fig. 1. The RTP crystal was cut with a trapezoidal geometry, and was placed inside the cavity of a conventional diode-pumped Q-switched Nd:YAG laser. Within this cavity, the fundamental 1064 nm field underwent TIR inside the RTP crystal, forming a folded cavity. The Stokes field also underwent TIR inside the RTP crystal, in a separate folded cavity formed by an independent pair of mirrors. The internal angles of the RTP trapezoid and the folding angles of the fundamental and Stokes resonators were designed to produce a polariton field which was generated at an incidence angle close-to-normal on the TIR surface. This enabled the terahertz radiation to be

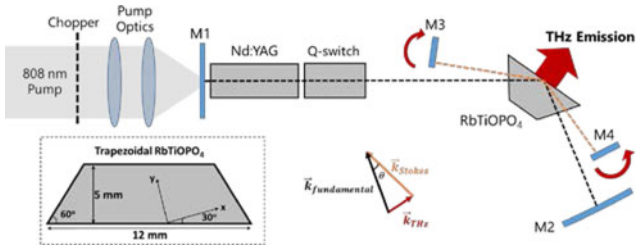

Fig. 1. Resonator layout for the THz polariton laser with intracavity RTP in a surface-emitting configuration.

directly refracted out of the RTP crystal. The internal angle θ between the fundamental and Stokes fields was adjusted to produce frequency-tunable THz radiation [12].

The fundamental resonator was end-pumped by a fiber coupled diode laser operating at 808 nm (100 μm core diameter, 0.22 NA; 10 W maximum output power). The diode laser was chopped at 200 Hz with a 50% duty-cycle to reduce thermal lensing. A pair of aspheric lenses produced a ~300 μm diameter pump spot inside a 1 at.% Nd:YAG crystal (5 mm length, 5 mm diameter; anti-reflection coated for 808 and 1064 nm). The fundamental resonator was 250 mm-long and was composed of a flat input mirror M1 ($T > 99\%$ at 808 nm and $R > 99.99\%$ at 1064 nm) and a concave output coupler M2 (radius of curvature = 1000 mm; $R = 99.4\%$ at 1064 nm). The fundamental field was Q-switched by an acousto-optic cell at a repetition rate of 3 kHz. This was substantially higher than the diode laser chopping frequency and hence was not affected by the chopped pump diode. The trapezoidal RTP crystal (Crystech Inc.) had base angle of 60° with longer base length of 12 mm, 5 mm height and 8 mm thickness in the crystallographic z axis direction. The orientation of the crystallographic xy plane with respect to the crystal geometry is shown inset in Fig. 1 and the laser fields were polarized in the z-direction. Total internal reflection of the fundamental and Stokes fields occurred at the uncoated long base of the trapezoid, and the crystal end faces were anti-reflection coated for the fundamental and Stokes wavelengths ($R < 0.3\%$ from 1060 to 1090 nm).

The pair of flat mirrors M3 and M4 were separated by 85 mm and coated for high reflectivity from 1060 to 1090 nm ($R > 99.99\%$ for M3 and $R > 99.9\%$ for M4) and formed the Stokes resonator. Each Stokes mirror was mounted on an independent rotation stage, which enabled high-precision tuning of the internal angle θ, and consequently fine adjustment of the THz frequency. To avoid clipping of the fundamental field when adjusting the Stokes resonator, both mirrors M3 and M4 were D-shaped.

The average fundamental field power leaking from M2 and the average Stokes power leaking from M4 were measured with a laser power meter, and their temporal characteristics were measured with a fast silicon photodiode. The wavelength of the fundamental and Stokes fields were monitored with a spectrometer, and the difference between the energy of these fields was used to calculate the terahertz frequency. The average terahertz output power was measured with the same apparatus described in [15], an optical chopper (10 Hz) and a Golay cell (Tydex GC-1T; 116.14 kV/W @10 Hz), in combination with a

long pass filter (Tydex, LPF 14.3) and a 50 mm focal length TPX lens (Tydex), to ensure that all the generated terahertz radiation was collected. The laser operated with the pump laser diode at 50% duty-cycle, and it is important to note that all the average output power levels presented in this manuscript are those obtained during the laser-on periods.

III. Results and Discussion

The fundamental resonator was optimized first, producing a 1064.4 nm field. Adjusting the interacting angle from $\theta = 1 - 2.8^\circ$, wavelength-tunable Stokes radiation from 1076.1 to 1087.5 nm was measured, corresponding to polariton fields from 3.05–5.98 THz being generated internally. For interacting angles below 1° the Stokes mirrors clipped the fundamental field, preventing oscillation of the fundamental field, and for angles above 2.8° no SPS fields could be detected, this being attributed to a decreasing overlap between the fundamental and Stokes cavity modes, resulting in decreasing SPS gain. The 2.8° upper limit for the interacting angle is below that observed for the linear resonator, in which SPS activity was present at angles as high as 3.6° inside RTP [15]. The frequency-coverage of the THz polariton laser based on RTP in linear (adapted from [15]) and in SE configurations are plotted in Fig. 2 for a 5.5 W diode pump input. In the figure, the average THz output power measured with the Golay cell, emitted from the TIR surface of the RTP crystal is plotted together with the average Stokes power measured leaking from M4. The SE resonator was continuously tunable in four regions, from 3.05–3.16 THz, from 3.50–4.25 THz, from 4.57–4.75 THz and from 5.40–5.98 THz, a substantially wider range when compared to the linear configuration in which terahertz detection was limited to 3.10–3.17 THz and 3.50–4.15 THz. The gaps in THz emission correspond to polariton modes in RTP located around 106, 143 and 161 cm^{-1} [15] and result from the increase in absorption close to resonance. It is important to note that the emission from RTP fills the emission gap from sources based on KTP and KTA [13], [14], and vice-versa. In the experimental setup, the output frequency was manually adjusted with the translation stages; this can be easily automated with motorized stages for rapid frequency scanning, envisioning future applications.

From Fig. 2 it should be noted that with the RTP in SE configuration, frequency-tunable THz radiation was detected for all interacting angles producing wavelength-tunable Stokes fields. This was not the case with the same crystal in linear configuration previously reported in [15], in which the highest detectable THz frequency was 4.15 THz, whilst frequencies as high as 7.05 THz were generated inside the nonlinear material. The frequency-tuning results obtained from the RTP in SE configuration confirms that extraction of the THz fields from the SPS crystal were the limiting factor for the linear configuration, and this can be avoided with the SE geometry. This is because the SE geometry virtually eliminates THz absorption losses for the fields generated at the TIR surface, producing measurable THz signal across the entire SPS tuning range.

The system was power scaled at the most efficient SPS frequency on each emitting band, 3.12 THz, 4.10 THz, 4.69 THz and 5.53 THz. The power scaling curves for the 4.10 THz, 1080.1 nm Stokes and 1064.4 nm fundamental (undepleted and depleted) fields are shown in Fig. 3, as a representation of the general power scaling response of the system. The undepleted fundamental field power corresponds to the 1064.4 nm output with the Stokes cavity blocked (i.e., no SPS action), and the depleted value correspond to the output leaking from M2 with the SPS process active (i.e., Stokes cavity unblocked). The decrease in power from the undepleted to the depleted fundamental field for a given diode pump level is related to the amount of energy channeled to the SPS process, and the percentage of depletion calculated from this difference in power is an indication of the SPS conversion efficiency [12].

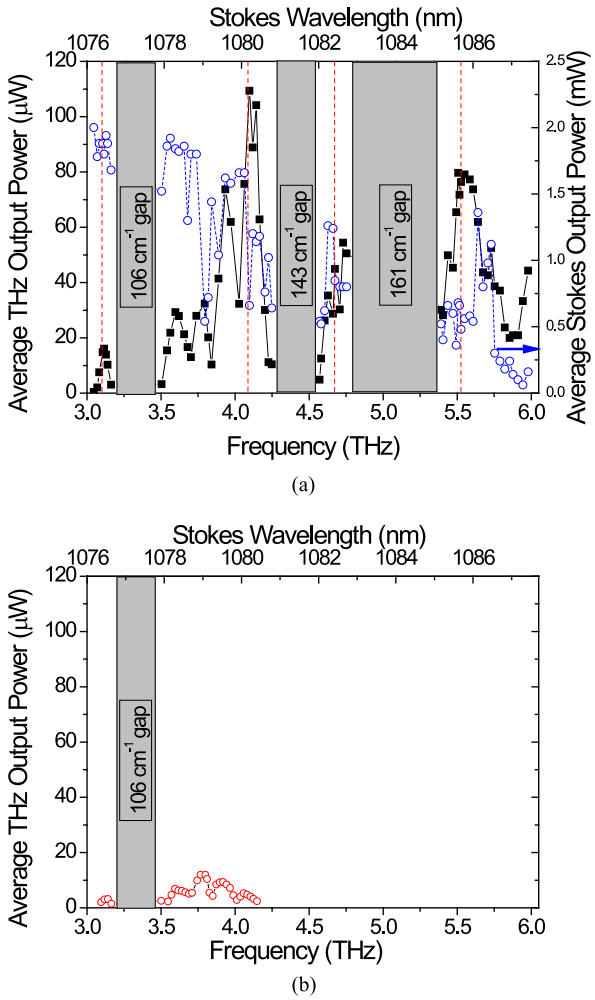

Fig. 2. Average THz output power and average Stokes power measured for a 5.5 W diode pump input (a) from the SE configuration. (b) From the linear configuration (adapted from [15]). The higher THz powers and expanded spectral coverage achieved by using the SE configuration are clearly apparent. The significant dips in THz power are attributed to water vapor absorption present in the laboratory environment [23].

Threshold for generating the fundamental field was 0.6 W diode pump power; while the lowest pump power required to achieve SPS threshold was 2.3 W, for a THz frequency of 4.10 THz (1080.1 nm Stokes). Considering the average output power at 1064 nm at this pump level (200 mW), the transmission of mirror M4 at 1064 nm (0.6%), the calculated cavity mode size inside the crystal (230 μm radius), and the measured pulse width

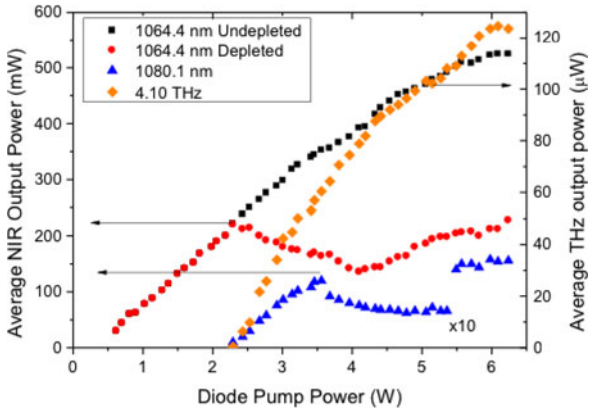

Fig. 3. Power scaling for the fundamental (undepleted and depleted), 1080.1 nm Stokes (magnified 10 times) and 4.10 THz fields.

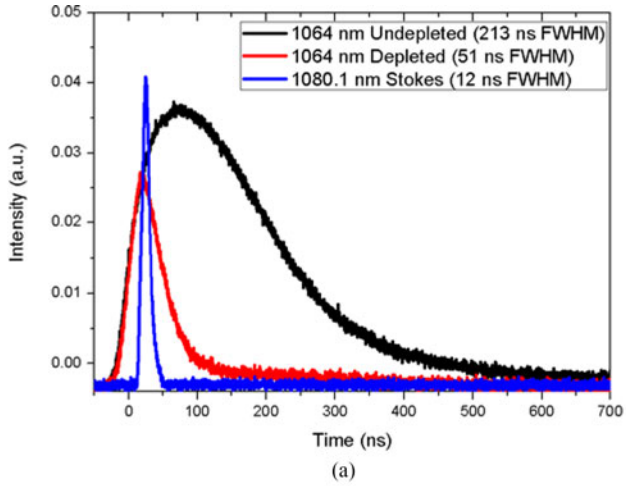

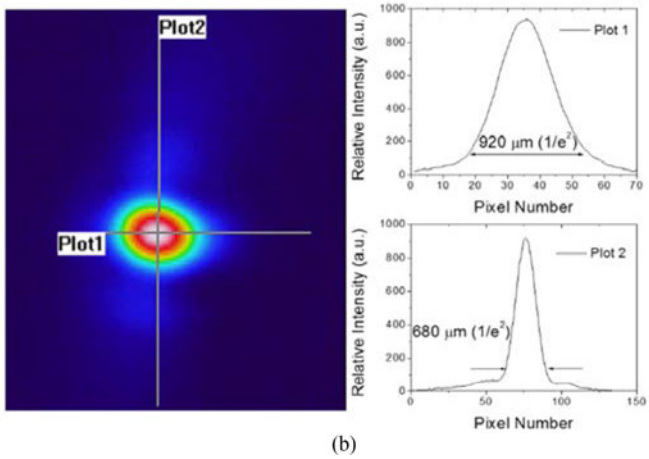

Fig. 4. (a) Temporal profiles of the depleted and undepleted 1064 nm, and 1080.1 nm Stokes fields at 6.0 W diode pump power; and (b) terahertz signal at 4.10 THz focused to a 920 × 680 μm spot (horizontal × vertical; 1/e^2) with a 50 mm focal length spherical lens into the THz camera.

at this pump level (270 ns full width half-maximum (FWHM)), a SPS threshold intensity of 27 MW/cm^2 can be calculated. This figure is comparable to that observed in other intracavity systems, which are typically lower than those observed in externally pumped resonators [12], [15], [18].

At 4.10 THz, a maximum average terahertz output power of 124.7 μW was measured for only 6.0 W diode pump power (pump depletion in excess of 60%), corresponding to a diode-to-THz conversion efficiency of 2.1 $\times$ 10^{-5}. This represents a 7-fold increase in power over the 16.2 μW previously obtained for the linear THz polariton laser [15], and one order of magnitude improvement in diode-to-THz efficiency, this demonstrating another great advantage of the SE configuration. The system maintained similar SPS thresholds and a high level of average output power at the other three frequencies evaluated, with a maximum average output power of 62.3 μW at 3.12 THz, 47.1 μW at 4.69 THz and 78.6 μW at 5.53 THz for a maximum 6.0 W diode pump input. The SPS threshold for the surface-emitting configuration is comparable to that of the linear cuboid crystal, suggesting similar gains for both configurations. Hence, the substantial increase in the THz signal detected from the surface-emitting configuration can be attributed to a much higher extraction efficiency. When comparing RTP with MgO:LN, the most explored SPS crystal, RTP yielded more than double the amount of THz output which suggests that the materials properties of RTP may be more favourable to nonlinear conversion via SPS. Moreover, in RTP laser damage to the TIR surface did not occur, as opposed to what at observed in MgO:LN, which required a protective Teflon coating to the TIR surface [21].

The temporal profile of the fundamental (undepleted and depleted) and 1080.1 nm Stokes fields were measured at 6.0 W diode pump as shown in Fig. 4. Close inspection of Fig. 4(a) shows that the rising edge of the Stokes pulse (blue line) coincides with the point at which depletion of the fundamental commences. The full-width at half maximum (FWHM) of the fundamental field pulse decreased from 213 ns undepleted to 51 ns when depleted, and the Stokes pulse width was measured to be 12 ns (FWHM). The area under the undepleted and depleted fundamental field pulses are related to the energy output of these fields, and the ratio between the pulse area of the depleted and undepleted pulses is another indication of the fundamental field depletion. From this ratio, a 65% depletion was calculated, a value comparable to that measured from the power scaling curves.

The linewidth of the free-running terahertz field was estimated from the coherence length of the 4.10 THz field, measured with a Fabry-Pérot interferometer [24] constructed from two silicon windows (0.5 mm thick, 50.8 mm diameter, Tydex). From the interferometric measurements, a coherence length of around 3.4 mm was measured, corresponding to a 28 GHz ($\pm$1 GHz) linewidth estimated at 4.10 THz, considering a Lorentzian spectrum [25]. This is similar to the free-running linewidth measured for other intracavity SPS systems, and could potentially be reduced with the insertion of etalons in the fundamental and Stokes cavities [19]. The polarization of the terahertz output was measured with a linear polyethylene polarizer (Tydex) to be vertically polarized, parallel to the crystal z-axis.

The terahertz output at 4.10 THz was collected with a 50 mm focal length TPX lens (Tydex) placed at $\sim$100 mm from the TIR surface, and focused on a camera sensitive to THz radiation

(IRV-T0831, NEC Corporation), as also shown in Fig. 4(b). A 920 × 680 μm (horizontal × vertical; 1/e^2; ±50 μm) spot was formed in the focal plane array of the camera, demonstrating the ability of the source to produce uniform and tightly-focused beams. The small asymmetry of the focused spot is a consequence of the ellipsoid mode shape at the TIR surface, and may be corrected with customized optics. The horizontal and vertical beam quality parameters (M^2) for the free-space propagating terahertz field at 4.10 THz was calculated with the knife-edge method, similarly to what was reported in [21], and assuming a close-to-Gaussian THz beam profile. From these measurements, horizontal and vertical beam quality parameters were calculated respectively to be $M_H^2 < 1.6$ and $M_V^2 < 1.1$. These values are substantially lower than that reported for an intracavity SPS laser in a linear configuration, using silicon prisms to extract the THz field, in which the beam quality was measured to be $M_H^2 \sim 6.7$ and $M_V^2 \sim 2.3$ [26], indicating that the SE configuration can increase the brightness of the THz output when compared to the linear configuration.

IV. Conclusion

In this manuscript we reported the development of the first THz polariton laser based on RTP in SE configuration. The combination of the good material properties of RTP in an intracavity surface-emitting configuration resulted in a record-high terahertz output, with an average output power of 124.7 μW detected at 4.10 THz. Furthermore, it was continuously tunable in four regions, from 3.05–3.16 THz, from 3.50–4.25 THz, from 4.57–4.75 THz and from 5.40–5.98 THz, significantly extending the frequency coverage of THz sources based on intracavity SPS, and filling the emission gaps of other nonlinear materials. The diode-to-THz conversion efficiency was 2.1×10^{-5}, the highest ever reported for an intracavity SPS laser, to the best of our knowledge. The horizontal and vertical beam quality parameters were $M_H^2 < 1.6$ and $M_V^2 < 1.1$, and the linewidth of the terahertz field was 28 GHz at 4.10 THz. When compared to the linear approach which uses silicon prisms to extract the THz fields, the surface-emitting configuration yielded a substantial increase in the range of terahertz frequencies detected and a notable increase in the average output power levels measured, this being a consequence of the superior extraction efficiency and the elimination of absorption losses for the THz fields generated at the TIR surface. Also, the M^2 parameters of the THz output in the horizontal and vertical directions were superior to what is typically obtained in the linear configuration. The results reported here suggest that the intracavity surface-emitting configuration is extremely advantageous, and represents a compelling advance towards producing practical THz sources with frequency-tunable output for real-world applications.

References

[1] A. R. Orlando and G. P. Gallerano, "Terahertz radiation effects and biological applications," *J. Infrared, Millim., THz Waves*, vol. 30, no. 12, pp. 1308–1318, 2009.

[2] A. J. Fitzgerald *et al.*, "Terahertz pulse imaging in reflection geometry of human skin cancer and skin tissue," *Phys. Med. Biol.*, vol. 47, pp. 3853–3863, 2002.

[3] S. J. Oh *et al.*, "Molecular imaging with terahertz waves," *Opt. Express*, vol. 19, no. 5, pp. 4009–4016, 2011.

[4] K. Kawase, Y. Ogawa, Y. Watanabe, and H. Inoue, "Non-destructive terahertz imaging of illicit drugs using spectral fingerprints," *Opt. Express*, vol. 11, no. 20, pp. 2549–2554, 2003.

[5] M. R. Leahy-Hoppa and M. J. Fitch, "Terahertz spectroscopy techniques for explosives detection," *Anal. Bioanal. Chem.*, vol. 395, pp. 247–257, 2009.

[6] J. Federici *et al.*, "THz imaging and sensing for security applications—Explosives, weapons and drugs," *Semicond. Sci. Technol.*, vol. 20, pp. S266–S280, 2005.

[7] M. Yahyapour, N. Vieweg, T. Göbel, H. Roehle, and A. Deninger, "Non-contact contact thickness measurements with terahertz pulses," in *Proc. World Conf. Non-Destruct. Test.*, 2016, pp. 1–8.

[8] S. Krimi *et al.*, "Highly accurate thickness measurement of multi-layered automotive paints using terahertz technology," *Appl. Phys. Lett.*, vol. 109, 2016, Art. no. 21105.

[9] R. K. May *et al.*, "Terahertz in-line sensor for direct coating thickness measurement of individual tablets during film coating in real-time," *J. Pharmaceutical Sci.*, vol. 100, no. 4, pp. 1535–1544, 2011.

[10] K. Kawase, J. Shikata, and H. Ito, "Terahertz wave parametric source," *J. Phys. D, Appl. Phys.*, vol. 35, no. 3, pp. R1–R14, Feb. 2002.

[11] S. Hayashi, K. Nawata, K. Kawase, and H. Minamide, "Terahertz parametric oscillator sources," in *Proc. OSA Tech. Digest*, 2014, Paper AW2A.1.

[12] A. Lee, Y. He, and H. Pask, "Frequency-tunable THz source based on stimulated polariton scattering in Mg:LiNbO$_3$," *IEEE J. Quantum Electron.*, vol. 49, no. 3, pp. 357–364, Mar. 2013.

[13] W. Wang *et al.*, "Terahertz parametric oscillator based on KTiOPO$_4$ crystal," *Opt. Lett.*, vol. 39, no. 13, pp. 3706–3709, 2014.

[14] W. Wang *et al.*, "THz-wave generation via stimulated polariton scattering in KTiOAsO$_4$ crystal," *Opt. Express*, vol. 22, no. 14, pp. 17092–17098, 2014.

[15] T. A. Ortega, H. M. Pask, D. J. Spence, and A. J. Lee, "Stimulated polariton scattering in an intracavity RbTiOPO$_4$ crystal generating frequency-tunable THz output," *Opt. Express*, vol. 24, no. 10, pp. 10254–10264, 2016.

[16] K. Kawase, J. Shikata, H. Minamide, K. Imai, and H. Ito, "Arrayed silicon prism coupler for a terahertz-wave parametric oscillator," *Appl. Opt.*, vol. 40, no. 9, pp. 1423–1426, 2001.

[17] T. Ikari, X. Zhang, and H. Minamide, "THz-wave parametric oscillator with a surface- emitted configuration," *Opt. Express*, vol. 14, no. 4, pp. 1604–1610, 2006.

[18] T. Edwards *et al.*, "Compact source of continuously and widely-tunable terahertz radiation," *Opt. Express*, vol. 14, no. 4, pp. 1582–1589, 2006.

[19] D. J. M. Stothard *et al.*, "Line-narrowed, compact, and coherent source of widely tunable terahertz radiation," *Appl. Phys. Lett.*, vol. 92, no. 14, pp. 3–5, 2008.

[20] Y. Wang *et al.*, "Energy scaling of a tunable terahertz parametric oscillator with a surface emitted configuration," *Laser Phys.*, vol. 24, no. 12, 2014, Art. no. 125402.

[21] T. Ortega, H. Pask, D. Spence, and A. Lee, "THz polariton laser using an intracavity Mg:LiNbO$_3$ crystal with protective teflon coating," *Opt. Express*, vol. 25, no. 4, pp. 1604–1610, 2017.

[22] A. Hildenbrand *et al.*, "Laser damage investigation in RbTiOPO$_4$ crystals: A study on the anisotropy of the laser induced damage threshold," *Laser-Induced Damage Opt. Mater.*, vol. 6403, 2006, Art. no. 64031W.

[23] I. Hosako *et al.*, "At the dawn of a new era in terahertz technology," *Proc. IEEE*, vol. 95, no. 8, pp. 1611–1623, Aug. 2007.

[24] A. Siegman, *Lasers*. Mill Valley, CA, USA: Univ. Sci. Books, 1986.

[25] I. V. Hertel and C. P. Schulz, "Coherence and photons," in *Atoms, Molecules and Optical Physics 2 (Graduate Texts in Physics)*. Berlin, Germany: Springer, 2015.

[26] D. Walsh, "Intracavity terahertz optical parametric oscillators," Doctoral dissertation, Univ. St. Andrews, St. Andrews, U.K., 2010.

Tiago A. Ortega was born and educated in Brazil. He received the Bachelor's degree in physics and the M.Sc. degree in applied physics from the University of Sao Paulo, Sao Carlos, Brazil, in 2007 and 2011, respectively. He is currently working toward the Ph.D. degree at Macquarie University, Sydney, N.S.W., Australia, working on the development of compact and frequency-tunable THz polariton lasers.

He worked on the development of solid-state lasers and optical systems for the medical industry from 2007 to 2014.

Mr. Ortega is the recipient of a scholarship from the Commonwealth of Australia under the Research Training Program scheme.

Helen M. Pask received the Ph.D. degree in physics from Macquarie University, Sydney, N.S.W., Australia, in 1992. She currently holds an Australian Research Council Future Fellowship at Macquarie University, with research interests in crystalline Raman lasers, THz generation and applications, remote sensing, and Raman spectroscopy.

David J. Spence was born in Birmingham, U.K., in 1975. He received the M.Phys. and D.Phil. degrees in physics from Oxford University, Oxford, U.K., in 1997 and 2001, respectively.

After a year in the industry and two years as a Research Assistant at Oxford, he moved to Sydney, Australia, in 2004. Following an Australian Research Council Postdoctoral Fellowship, he won a Lectureship at Macquarie University, Sydney, N.S.W., Australia, where he is currently an Associate Professor. His research interests include lasers and nonlinear optics, including Raman lasers and frequency conversion, and visible and ultraviolet laser materials.

Andrew J. Lee received the Bachelor's degree (Honors First Class) in opto-electronics and the Ph.D. degree in physics from Macquarie University, Sydney, N.S.W., Australia, in 2001 and 2007, respectively.

He is currently a Macquarie University Vice-Chancellors Innovation Fellow with Macquarie University. His current research interests include development of high-power THz sources and their applications, development of high-power continuous wave Raman lasers, and vortex lasers.